

# Potent antimicrobial activity of bone cement encapsulating silver nanoparticles capped with oleic acid

Polina Prokopovich,<sup>1,2,3</sup> Mathias Köbrick,<sup>1,2</sup> Emmanuel Brousseau,<sup>2</sup> Stefano Perni<sup>1,3</sup>

<sup>1</sup>School of Pharmacy and Pharmaceutical Sciences, Cardiff University, Cardiff CF10 3NB, Wales, UK

<sup>2</sup>Institute of Mechanical and Manufacturing Engineering, School of Engineering, Cardiff University, Cardiff CF24 3AA, Wales, UK

<sup>3</sup>Department of Biological Engineering, Massachusetts Institute of Technology, Cambridge, Massachusetts

Received 30 January 2014; revised 19 April 2014; accepted 21 April 2014

Published online 00 Month 2014 in Wiley Online Library (wileyonlinelibrary.com). DOI: 10.1002/jbm.b.33196

**Abstract:** Bone cement is widely used in surgical treatments for the fixation for orthopaedic devices. Subsequently, 2–3% of patients undergoing these procedures develop infections that are both a major health risk for patients and a cost for the health service providers; this is also aggravated by the fact that antibiotics are losing efficacy because of the rising resistance of microorganisms to these substances. In this study, oleic acid capped silver nanoparticles (NP) were encapsulated into Poly(methyl methacrylate) (PMMA)-based bone cement samples at various ratios. Antimicrobial activity against Methicillin Resistant *Staph-*

*lococcus aureus*, *S. aureus*, *Staphylococcus epidermidis*, *Acinetobacter baumannii* was exhibited at NP concentrations as low as 0.05% (w/w). Furthermore, the mechanical properties and cytotoxicity of the bone cement containing these NP were assessed to guarantee that such material is safe to be used in orthopaedic surgical practice. © 2014 Wiley Periodicals, Inc. *J Biomed Mater Res Part B: Appl Biomater* 00B:000–000, 2014.

**Key Words:** bone cement, antimicrobial, silver nanoparticles, nanoindentation, PMMA

**How to cite this article:** Prokopovich P, Köbrick M, Brousseau E, Perni S. 2014. Potent antimicrobial activity of bone cement encapsulating silver nanoparticles capped with oleic acid. *J Biomed Mater Res Part B* 2014:00B:000–000.

## INTRODUCTION

Bone cement is a biomaterial routinely used during orthopaedic surgeries to accomplish fixation between bone and an orthopaedic device. Microbial infections are a serious risk associated with any type of surgical procedure; according to the National Healthcare Safety Network data the infection rates as a result of the total joint replacements (TJR) surgeries are between 1.7–2% in the UK<sup>1</sup>, while it reaches up to 2.3% in the United States<sup>2</sup> with the highest rate for ankle replacement (15%).<sup>3</sup>

The traditional approach to prevent infections caused by the implantation of bone cement is through the use of antibiotics either through parental delivery<sup>4,5</sup> or through release from the bone cement itself.<sup>6–10</sup> However, the reliance on antibiotic therapies appears to be a time-limited solution because of the continuing increase of microorganisms resistance to these molecules.<sup>11,12</sup> Hence, the development of antimicrobial therapies or prophylactic treatments not based on antibiotics is of particular interest and extremely urgent. The utilization of nanometals, particularly silver,<sup>13</sup> is a promising example of such alternative approaches.

Although metal nanoparticles (NP) have been synthesized by a variety of physical and chemical protocols, it is the reduction of metal salts that has become the standard route for their synthesis. For instance, to prepare silver NP, ionic silver ( $\text{Ag}^+$ )

contained in a salt, generally  $\text{AgNO}_3$ , is reduced to metal silver ( $\text{Ag}^0$ ) through a reducing agent such as  $\text{HNO}_3$ /citrate,<sup>14</sup> Al-alkoxide,<sup>15</sup>  $\text{NaBH}_4$ ,<sup>16</sup> *N,N*-dimethyl formamide,<sup>17</sup> or sugars.<sup>18</sup> The NP can also be stabilized using chelating substances such as: citrates,<sup>19</sup> oleic acid,<sup>18</sup> and glutamic acid<sup>20</sup> or prepared with a capping agent that allows binding of other compounds to the NP such: glutathione,<sup>21,22</sup> cysteine,<sup>22,23</sup> or tiopronin.<sup>24</sup> Moreover, silver NP of different morphologies (size and shape) can be obtained modifying the reaction conditions.<sup>25</sup>

In this work, silver NP capped with oleic acid were prepared using a modified Tollens method<sup>18,26</sup> and characterized; this was followed by their encapsulation in Poly(methyl methacrylate) (PMMA)-based bone cement at different concentrations. The obtained formulations of bone cements were analyzed for their antimicrobial activity against Methicillin Resistant *Staphylococcus aureus* (MRSA), *S. aureus*, *Staphylococcus epidermidis*, and *Acinetobacter baumannii*. Also cytocompatibility and material characterisation of these bone cement materials were performed.

## MATERIALS AND METHODS

### Silver-oleic acid stabilized NP preparation and characterization

**Chemicals.**  $\text{AgNO}_3$  ( $\geq 99.0\%$ ), sodium hydroxide (99+%), aqueous ammonia ( $\text{NH}_3$ ), oleic acid (99+%), and glucose were supplied by Sigma Aldrich.

**Correspondence to:** Dr. P. Prokopovich (e-mail: prokopovichp@cf.ac.uk)

Contract grant sponsor: Arthritis Research UK; contract grant number: ARUK:1846

**Synthesis of particles.** The Ag NPs synthesis was performed following a modified Tollens technique as proposed by Le et al. (2010).<sup>18</sup> In particular, silver nitrate (1.7 g, 0.10 mmol) was dissolved in deionized water (100 mL), this was followed by Ag<sub>2</sub>O precipitation in the presence of NaOH (0.62g, 0.15mmol). The obtained precipitate was filtered and dissolved in aqueous ammonia (100 mL, 0.4%, w/w) until the transparent solution of [Ag(NH<sub>3</sub>)<sub>2</sub>]<sup>+</sup><sub>(aq)</sub> formed. Oleic acid (2.5g, 8.9 mmol) was added drop wise into the complex with vigorous stirring that was continued for 2 h at room temperature until complete homogeneity of the reaction mixture was achieved. Glucose (2 g, 0.11mmol) was added to the mixture at room temperature with gentle stirring. The reduction process of the silver complex solution (in a quartz glass) was initiated with UV irradiation (UV lamp ( $\lambda = 365$  nm, 35 W)). UV treatment was carried out for 8 h under vigorous stirring without additional heating. After 8 h of irradiation, a transparent dispersion of oleic acid-stabilized Ag NPs was obtained.

**Transmission electron microscopy—size distribution.** For transmission electron microscopy (TEM) characterisation, a 4  $\mu$ L droplet of NP suspension was placed on a plain carbon-coated copper TEM grid and allowed to evaporate in air under ambient laboratory conditions for several hours. Bright field TEM images were obtained using a JEOL-1010 microscope at 80 kV equipped with a Gatan digital camera. Typical magnification of the images was 100,000 $\times$ . Images were analyzed with the computer software ImageJ and the diameters of at least 150 particles were determined.

#### Encapsulation of AgNP stabilized with oleic acid into orthopaedic bone cement and its mechanical characterisation

The silver-oleic acid stabilized NP were mixed with PMMA-based bone cement powder to achieve 0.1, 0.05, and 0.01% (w/w) silver concentration in the cement. The mixture was subsequently inserted into a mould at approximate dough time of 1 min. The filled mould was pressed between two glass plates for 1 h. After the cement had hardened, it was pushed out from the mould and stored under dark, sterile conditions at room temperature. All assays were performed on cylindrical specimens (6 mm in diameter and 12 mm in height). Prior to testing all bone cement specimens were conditioned at 37°C for 24 h.

**Compression testing of PMMA-based composite bone cement.** Compression tests were undertaken on the Zwick Roell ProLine table-top Z050/Z100 materials testing machine according to BS ISO 5833:2002. The compression tests were conducted at a constant cross-head speed of 20.0 mm/min to produce a curve of displacement against load. For each specimen, the compressive strength of the bone cement was determined by dividing the force applied to cause fracture by the original cross-sectional area of the cylinder. The average compressive strength of five specimen was calculated.

**Atomic force microscope nanoindentation of PMMA-based composite bone cement.** An atomic force microscope (XE-100 Advanced Scanning Probe Microscope from Park Sys-

tems, Korea) was used for nanoindentation tests. These were performed using a DNSIP probe (Bruker; spring constant = 181 N/m) made of a rectangular stainless steel cantilever and a 3-sided diamond tip having a nominal height of 50  $\mu$ m and a nominal tip radius of 40 nm. The nanoindentation was performed at various applied loads: 5, 15, 25, 35, and 45  $\mu$ N. Each indentation had a holding time of 10 sec and a speed (loading rate) of 300 nN/s. For each loading force at least four measurement points were chosen on the sample. The nanoindentation tests were performed after immersion of the bone cement specimen in phosphate buffer solution (PBS) for 0 h, 24 h, 2 weeks, and 4 weeks. Thus, for each silver concentration, at least 100 nanoindentation cycles were conducted during this study. The mechanical properties were calculated from the obtained unloading curves according to the Oliver and Pharr method.<sup>27,28</sup> First, the unloading curve was fitted with the following equation:

$$F = \alpha (h - h_{\max})^m \quad (1)$$

Where:

$h$  is the penetration depth,  $\alpha$ ,  $h_{\max}$ , and  $m$  are fitting parameters.

Then the Young's modulus ( $E$ ) at a penetration depth equal to  $h_{\max}$  was calculated as:

$$E = \pi^2 \frac{S}{2} \sqrt{A} \quad (2)$$

Where:

the stiffness ( $S$ ) was given by:

$$S = \left. \frac{dF}{dh} \right|_{h=h_{\max}} \quad (3)$$

and the area of the indenter contact ( $A$ ) was estimated as:

$$A = 24.5 \left( h_{\max} - 0.72 \frac{F_{\max}}{S} \right)^2 \quad (4)$$

**Determination of antimicrobial activity of PMMA-based composite bone cement.** The antimicrobial activity of the bone cement samples was tested using the method adopted from Bechert et al. (2000)<sup>29</sup> using three Gram-positive bacteria: MRSA NCTC 12493, *S. aureus* NCIMB 9518, *S. epidermidis* RP62a and one Gram negative: *A. baumannii* NCTC 9214. The microorganisms were cultured in Brain-Heart Infusion (BHI) broth at 37°C for 24 h. Bone cement samples with different concentrations of silver-oleic acid capped NP were placed into 24-well plate. The experiment was performed in duplicate on three independent cultures (6 in total). Microbial suspension of 2.5 mL were added to each well to cover the bone cement sample and incubated at 37°C for 1 h to allow microorganisms to adhere to the cement. After 1 h the microbial suspension was removed and the cement was rinsed three times with PBS. 1 mL of 1/10 BHI (dilution with PBS) was added in each well and the plate was incubated at 37°C for 24 h. During this phase,

the microorganisms adhering to the cement detached. From each well 50  $\mu\text{L}$  of the bacterial suspension was transferred in another 100-well plate (Bioscreen C accessories, Labsystems, Finland) where each well contained 100  $\mu\text{L}$  of fresh BHI broth. This plate was then incubated in a plate reader (Bioscreen C analyser, Labsystems, Finland) at 37°C and the growth curves in each well were recorded through measuring optical density at 600 nm every 15 min for 24 h. The microbial growth curves were fitted with the Baranyi–Roberts model [Eq. (5)–(7)] to estimate the duration of the lag phase ( $\lambda$ ) and the maximum growth rate ( $\mu_{\text{max}}$ ).

$$y(t) = y_0 + \mu_{\text{max}} A(t) - \ln \left( 1 + \frac{e^{\mu_{\text{max}} A(t)} - 1}{e^{(y_{\text{max}} - y_0)}} \right) \quad (5)$$

where:

$$A(t) = t + \frac{1}{\mu_{\text{max}}} \ln(e^{-\mu_{\text{max}} t} + e^{-h_0} - e^{-\mu_{\text{max}} t - h_0}) \quad (6)$$

and:

$$h_0 = \mu_{\text{max}} \lambda \quad (7)$$

**In vitro cytotoxicity studies of PMMA-based composite bone cement.** Osteoblast cells (MC-3T3) were cultured in Dulbecco's Modified Eagle's Medium supplemented with foetal bovine serum (10%, v/v); cells were incubated at 37°C in humidified atmosphere with 5%  $\text{CO}_2$ . Cells were grown till confluence, washed twice with sterile PBS, and detached with trypsin; osteoblast cells were counted (using trypan blue to differentiate between viable and no-viable cells) and diluted to a concentration 10<sup>5</sup> cells/mL with fresh medium.

Bone cement samples were sterilized with 70% alcohol and washed thrice with sterile PBS prior to use. Samples were placed in 24-well plate containing 2 mL of osteoblast cells suspension prepared as described earlier. Osteoblasts were incubated with the bone cement at 37°C in humidified atmosphere with 5%  $\text{CO}_2$ . After 2 days the bone cement samples were transferred to a clean 24-well plate with 2 mL of fresh medium without red phenol. Osteoblast cells viability was assessed using the MTT assay kit (Invitrogen, UK). The MTT solution was prepared according to the manufacturer guidelines and 10  $\mu\text{L}$  added to each well. After incubation for 2 h at 37°C in humidified atmosphere with 5%  $\text{CO}_2$ , the samples were transferred in a new 24-well plate and the MTT solubilisation solution added; when full dissolution of the crystals occurred, 100 mL of liquid was transferred in a 96-well plate where the absorbance of each samples was read at 570 nm. Results are presented as the average and standard deviation of three independent bone cement samples.

**Silver release studies from PMMA-based composite bone cement.** The silver ion release from bone cement samples was determined by inductively coupled plasma-mass spectroscopy analysis (Perkin Elmer Optima 2100DV OES)

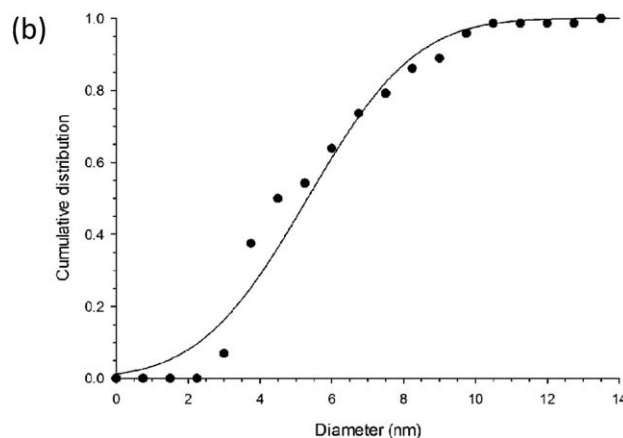
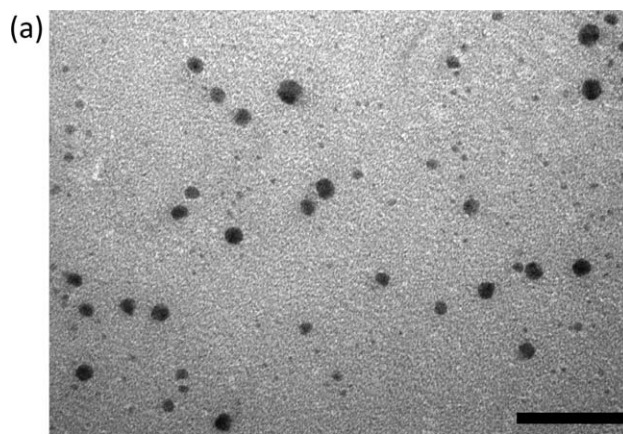


**FIGURE 1.** TEM images (Bar equals to 50 nm) (a) and cumulative distribution of diameters (b) of silver-oleic acid capped NP. Solid points are experimental data and continuous line is Gaussian fitting.

against the Primar 28 element standard, which had silver at a concentration of 100 mg/L from which subsequent dilutions were made. Samples of bone cement were placed in 10 mL of fresh sterile PBS and incubated at 37°C for 7 days with a daily change of immersion liquid. Silver ion release was measured daily.

#### Statistical analyses

ANOVA and *t*-test were performed on the results using SPSS (12.0). For all analyses,  $p < 0.05$  was considered statistically significant.

#### RESULTS

Example of TEM images of the silver NP are shown in Figure 1(a). All particles appeared rounded with an average diameter of  $5.3 \pm 2.3$  nm; the cumulative distributions of the NP diameters are presented in Figure 1(b). The distributions are closely modeled by a normal (Gaussian) distribution.

The antimicrobial properties of the bone cements embedded with the silver NP were determined through the lag phase and growth rate of the MRSA, *S. aureus*, *S. epidermidis*, and *A. baumannii* survivors detached from the bone cement samples. Examples of these curves are shown in

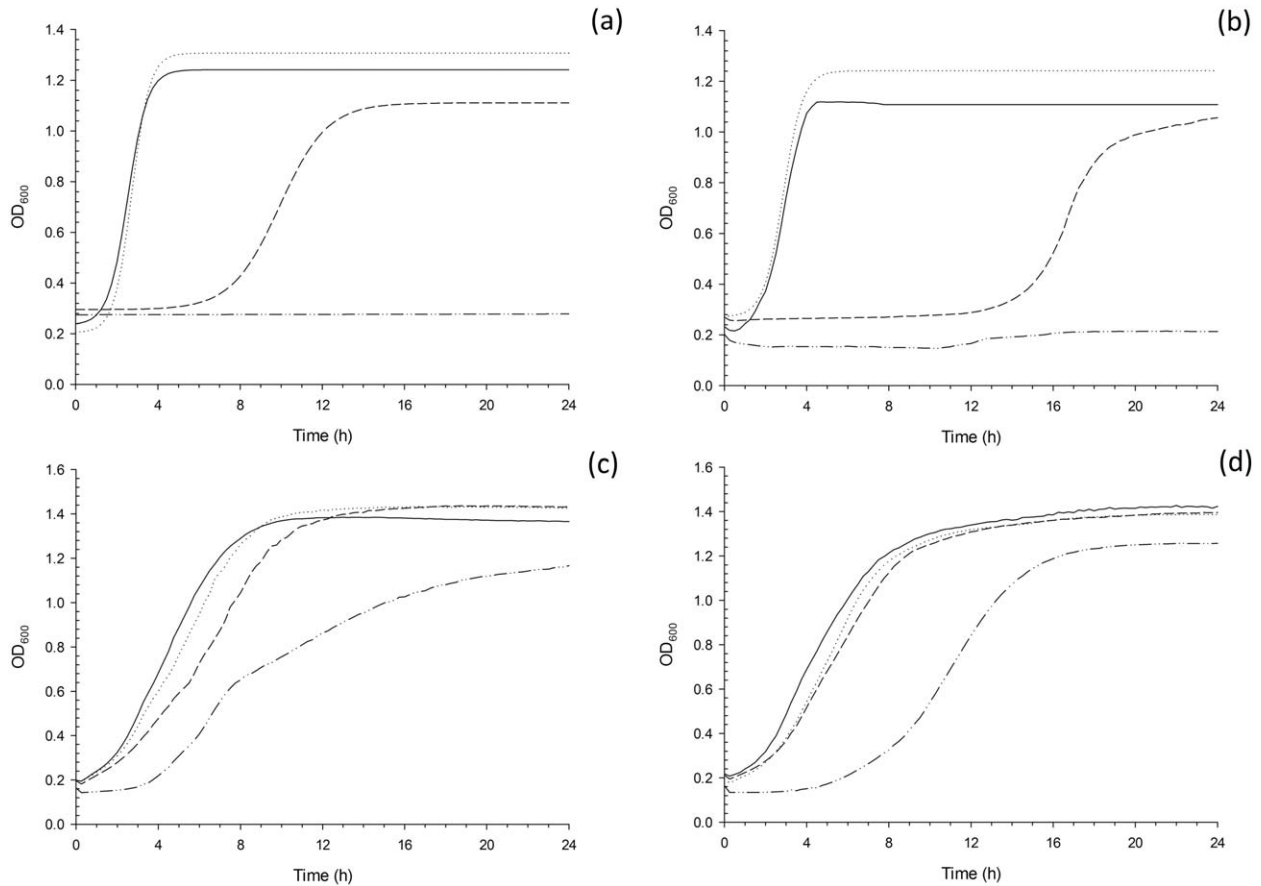


**FIGURE 2.** Examples of growth curve of *S. aureus* (a), MRSA (b), *S. epidermidis* (c), and *A. baumannii* (d) survivors on bone cement containing Ag NP in different amounts (w/w). 0%, 0.01%, 0.05%, 0.1%.

Figure 2; while the growth rate and lag phase of the growth curves fitting with the Baranyi model are presented in Table I. For samples without NP the OD<sub>600</sub> of the solution starts

**TABLE I. Lag Phase and Growth Rate of the Growth Curves of Survivals on Bone Cement Containing Ag Nanoparticles Capped with Oleic Acid**

	Concentration	$\lambda$ (h)	Growth Rate (h <sup>-1</sup> )
	of Ag Nanoparticles (% w/w)		
<i>S. aureus</i>	0	2.65 ± 0.10	2.10 ± 0.09
	0.01	2.48 ± 0.31	2.18 ± 0.18
	0.05	14.79 ± 1.54	0.85 ± 0.15
	0.1	> 24	
MRSA	0	2.21 ± 0.28	2.41 ± 0.23
	0.01	2.38 ± 0.20	2.37 ± 0.21
	0.05	12.08 ± 1.78	0.81 ± 0.10
	0.1	> 24	
<i>S. epidermidis</i>	0	3.42 ± 0.49	0.74 ± 0.03
	0.01	3.14 ± 0.10	0.66 ± 0.06
	0.05	4.91 ± 0.32	0.53 ± 0.06
	0.1	6.75 ± 0.33	0.28 ± 0.06
<i>A. baumannii</i>	0	2.93 ± 0.30	0.50 ± 0.08
	0.01	3.93 ± 0.47	0.57 ± 0.04
	0.05	4.20 ± 0.04	0.47 ± 0.02
	0.1	9.81 ± 0.43	0.55 ± 0.03

Mean ± standard deviation

increasing after about 1–2 h and reached a plateau after 4 h for *S. aureus* and MRSA. *S. epidermidis* and *A. baumannii* curves exhibited a similar lag phase, but they reached a plateau only after about 10–12 h. Bone cement impregnated with 0.01% of NP returned the same growth curves as the controls; therefore, no antimicrobial effect was detected at this concentration. This is confirmed with the results presented in Table I, where it can be seen that both the lag phase and the growth rate at 0.01% (w/w) Ag NP did not show significant differences with the control samples ( $p > 0.05$ ). However, the lag phase of all four bacteria increased compared to the control samples ( $p < 0.05$ ), when the concentration of silver in the bone cement was increased to 0.05% (w/w); while the growth rate decreased ( $p < 0.05$ ). For samples containing 0.1% (w/w) of silver NP the lag phase increased further ( $p < 0.05$ ) and for *S. aureus* and MRSA no growth was evident after 24 h.

The possibility of silver NP having a cytotoxic effect was investigated through the MTT assay on osteoblast cells (Figure 3). The presence of silver NP in bone cement did not impact on the outcome of the enzymatic activity tested by the MTT ( $p > 0.05$ ) as all samples returned a OD<sub>540</sub> of about 0.4 a.u. of the solution containing the dissolved formazan.

The bone cement loaded with Ag NP released Ag<sup>+</sup> ions to the surrounding fluid (Figure 4). The cumulative amount of Ag<sup>+</sup> ions released from the samples containing



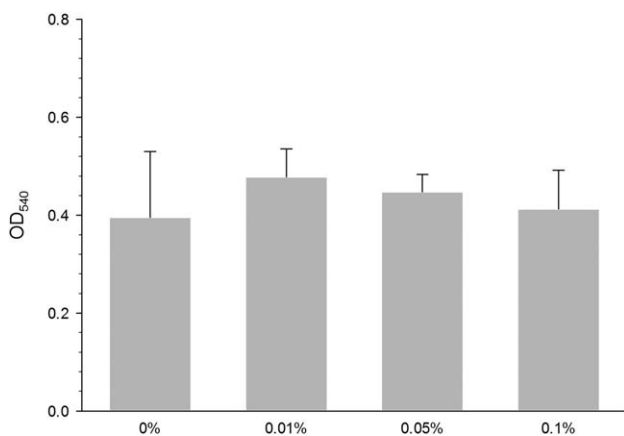


FIGURE 3. MTT assay for bone cement containing NP.

0.05 and 0.1% of silver NP increased monotonically from day 1 to day 7 for all samples and no difference was detected between the two ( $p > 0.05$ ). The bone cement containing 0.01% of Ag NP released smaller amount of silver ions than the other samples and the concentration of  $\text{Ag}^+$  did not increase after 3 days [Figure 4(a)]. The corresponding kinetics of silver ions released is shown in Figure 4(b) where it is evident that the release is faster at the beginning of the contact with fluid and slowly decreases with time.

Figure 5 shows the changes of the calculated Young's modulus over a 4 week period for the different concentrations of silver NP determined through nanoindentation tests. For a given concentration of silver NP, Young's moduli generally exhibited consistent values on the surface and in the bulk of the samples; bone cement specimen containing silver NP at low concentration (0.01%, w/w) displayed Young moduli not dissimilar from the control samples irrespectively of the immersion time in PBS. The immersion in PBS did not affect the Young moduli measured for the control samples and for bone cement containing 0.01% silver NP. At higher silver NP concentrations (0.05 and 0.1%, w/w), the Young moduli determined for the bone cement samples were higher than the control just after preparation ( $t = 0$  h); this difference slowly disappeared after immersion in PBS.

The amount of fluid absorbed by the bone cements resulted in an augmentation of the weight of the samples (Figure 6). In particular, this weight increased significantly during the first 2 weeks and after that, the amount of fluid in the samples remained stable. No difference in these results was observed between the different concentrations of silver NP encapsulated in bone cement over time.

The mechanical properties of the bone cement with silver NP embedded were assessed through the compression strength (Figure 7) over period of 3 months. Bone cement without any NP had compression strength of  $98 \pm 9$  MPa, while the presence of these NP did not have a significant impact of the resistance to compression compared to control samples without NP ( $p > 0.05$ ). Also no changes in compression strength were observed after 3 months in PBS ( $p > 0.05$ ).

## DISCUSSION

A synthesis method using the Tollens process has been proposed for synthesizing Ag NPs with controlled size.<sup>26</sup> The basic reaction in this process involves the reduction of a silver ammonia solution by using either aldehydes or reducing sugars.<sup>30</sup> In comparison with other Tollens methods, that require the use of toxic solvents and highly reactive chemical-reducing agents, this technique is simple and inexpensive. The antimicrobial activity of the silver NP used in this work was assessed through the duration of the lag phase of the growth curve displayed by the bacteria remaining on the bone cement after contact; as described in Bechert et al. (2000)<sup>29</sup> and Prokopovich et al. (2013),<sup>24</sup> this lag phase is more correctly denoted as "apparent lag phase" and is related to the number of living cells surviving on the bone cement samples, the higher the bacteria concentration the shorter the apparent lag phase.

The results (Table I) presented here demonstrated that the lowest concentration of NP (0.01%, w/w) is ineffective against all pathogenic species used in this study. Increasing the concentration returned progressively higher levels of

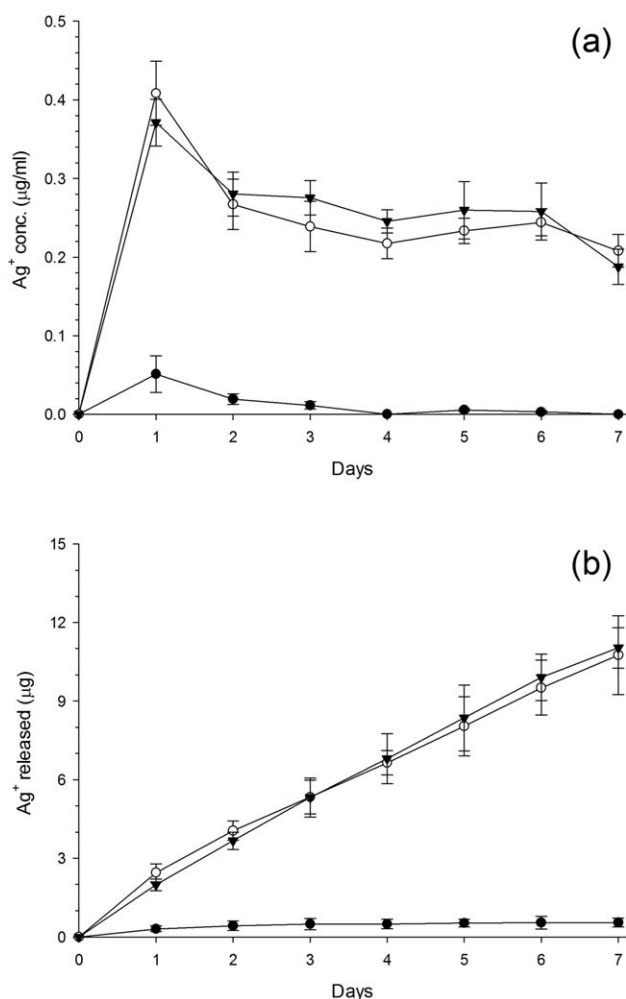
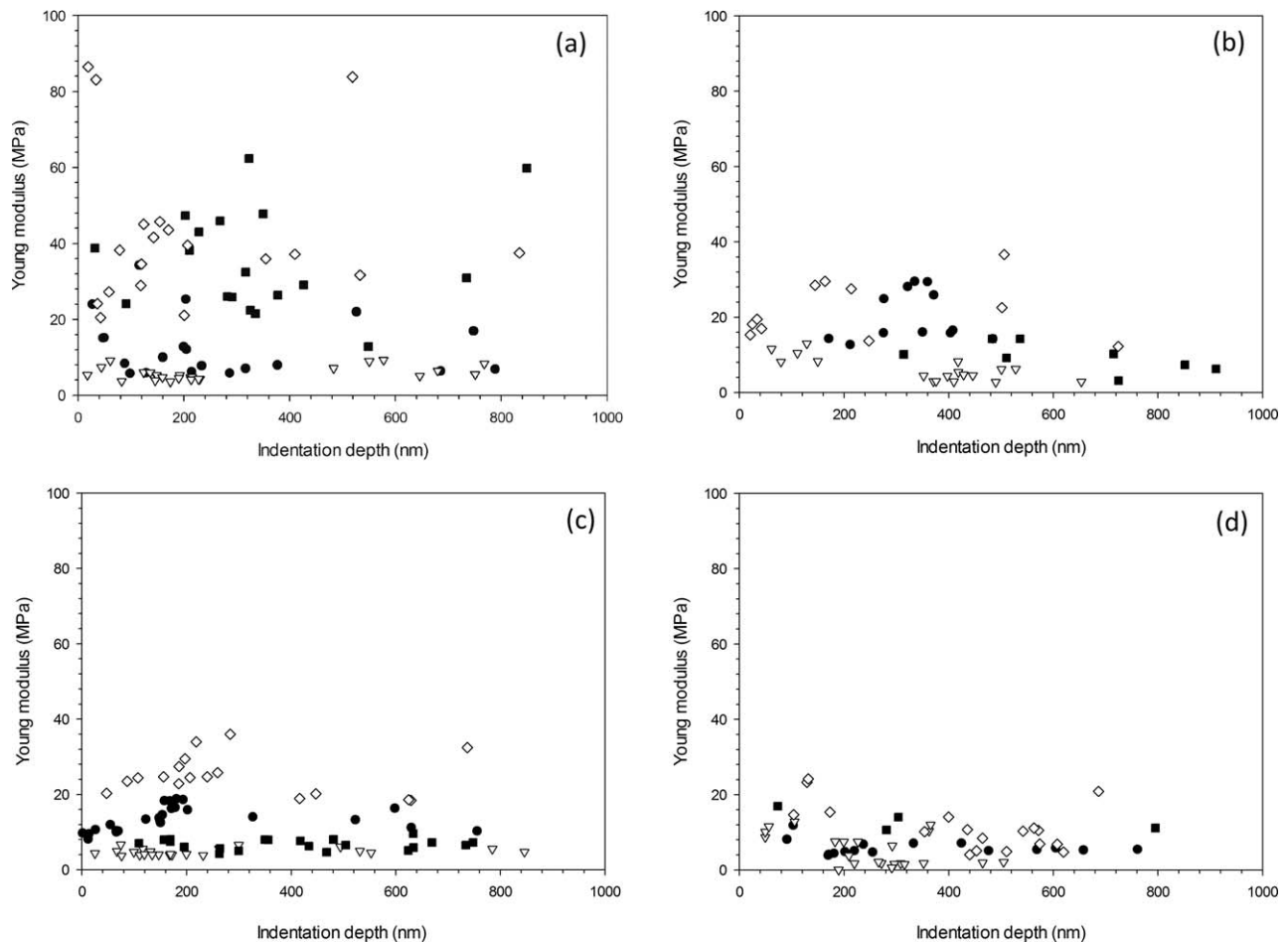


FIGURE 4. Releases of silver ions from bone cement. Concentration in the release medium (a) and cumulative release (b). (●) 0.01%, (○) 0.05%, and (▼) 0.1%.



**FIGURE 5.** Young modulus of bone cement containing NP determined through nanoindentation tests after immersion in PBS for 0 h (a), 24 h (b), 2 weeks (c), and 4 weeks (d). (●) 0%, (▽) 0.01%, (■) 0.05%, and (◇) 0.1%.

antimicrobial activity with differences between strains. *S. aureus* and MRSA were totally removed by silver NP at concentrations of 0.1%, w/w, while the longer “apparent lag phase” of MRSA with concentrations of 0.05% highlighted the greater vulnerability of MRSA to silver NP. Our results also suggested that *S. epidermidis* and *A. baumannii* were more resistant to silver NP than both *S. aureus* strains used in this work as little effect was detected in bone cement samples containing 0.05%, w/w of silver NP and living cells were detected in samples impregnated with silver NP at a concentration of 0.1%, w/w (Figure 2). However, the observed reduction of *A. baumannii* and *S. epidermidis* proved that the encapsulation of oleic acid capped silver NP in bone cement can be a viable approach to prevent infections offset. The pathogens tested in our work are representative of the most commonly found causes of infections in postoperative surgeries,<sup>31,32</sup> particularly *A. baumannii* is receiving a lot of attention in virtue of its resistance to many of the drugs generally utilized to treat orthopaedic surgeries related infections.<sup>33</sup> Some of *S. epidermidis* strains also possess high resistance to gentamicin; in addition, some *S. epidermidis* isolates have shown resistance to Methicillin (so called Methicillin Resistant *S. epidermidis* or MRSE) and the strain used in this work (RP62a, also known as ATCC 35984) is one of these.<sup>34</sup>

The high antimicrobial activity of bone cement containing oleic acid capped silver NP against the most common source of postoperative infections, which are also increasingly resistant to the routinely used antibiotics to treat them, highlights the significant benefit of such approach in preventing infection offset in patients undergoing surgeries requiring bone cement.

Another form of silver NP was used by Alt et al. (2004),<sup>35</sup> however, the properties of the nanomaterial used in that study were not characterized further than the average size (5–50 nm), furthermore no description of the synthetic method was given and the NP were generally referred as “nanosilver.” Growth of MRSA and MRSE was not prevented by PMMA bone cement containing nanosilver at concentration of 0.1%, w/w,<sup>35</sup> hence that type of silver NP was not as effective as oleic acid capped silver NP because such concentration is capable of reducing the number of viable cells of these two species (Figure 2). Other silver NP (tiopronin capped and in two different sizes) were used in previous studies to confer antimicrobial activity to PMMA bone cement and they did show a total reduction of living MRSA at concentrations as low as 1%, w/w even for the most active type.<sup>24</sup> Therefore, the silver NP used here, capped with oleic acid, appeared to display higher lethality toward microorganisms compared to tiopronin capped ones. Not

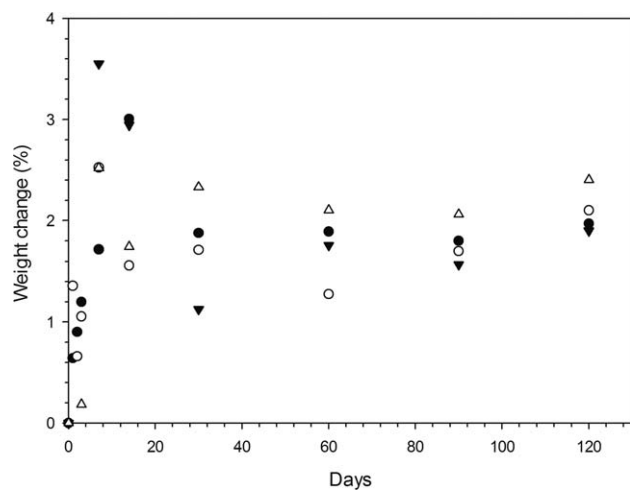


**FIGURE 6.** Percentage of weight variation of bone cement containing NP nanoindentation after immersion in PBS (a). (●) 0%, (▽) 0.01%, (■) 0.05%, and (△) 0.1%.

only silver NP have been encapsulated in bone cement to help infections offset; other nanomaterials such as: chitosan NP,<sup>36</sup> quaternised chitosan derivative,<sup>34</sup> and mesoporous silica NP<sup>37</sup> along with Nisin-F (a bacteriocin)<sup>38</sup> and silver ions<sup>39</sup> were used with various degree of success. However, in these studies the amount of antimicrobial compound added to the bone cement was significantly higher than 0.05 and 1%, w/w used here, in some cases up to 20%, w/w<sup>34</sup> and 30%.<sup>36</sup> Such differences starkly highlight the potent antimicrobial activity of the oleic acid capped silver NP compared to other antibacterial compounds.

Many properties of the NP are important in determining the antimicrobial activity, for example: size and shape have been linked to different bactericidal activity<sup>40</sup>; furthermore, the amount and chemical nature of capping agent have also been implicated in varying antimicrobial activity among NP.<sup>24</sup> A higher percentage of capping agent reduced the NP capacity of preventing bacteria growth,<sup>24</sup> however, the different synthetic conditions used to obtain NP with dissimilar quantity of capping agent also resulted in NP of different

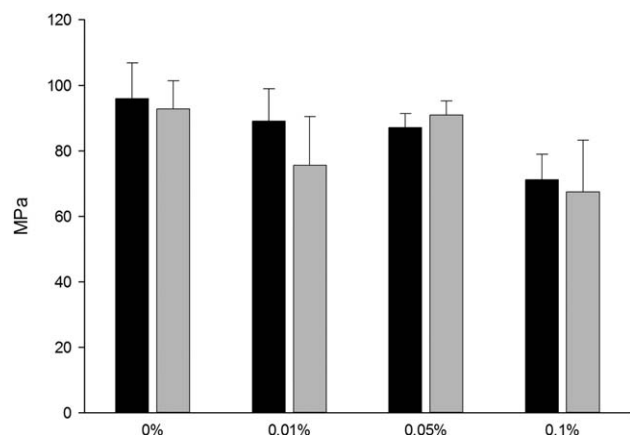


**FIGURE 7.** Compression strength of bone cement containing NP after 0 h (black column) and 3 months (light gray column)

mean size, hence the impact of size and organic fraction present in the NP (capping agent) could not be univocally assessed. Interestingly, the size of the tiopronin capped NP that did not exhibited any antimicrobial activity (about 5 nm)<sup>24</sup> is similar to the size of NP prepared here, thus, it can be said that size alone is not a unique factor granting antimicrobial activity to silver NP. In addition, it has been suggested that the amount of silver ions released in the surrounding media by silver NP is not the only mechanism of action of such nanomaterials for inactivating microorganisms.<sup>22,24</sup> The results presented here (Figure 4) coupled with those presented in Prokopovich et al. (2013)<sup>24</sup> further strengthen such conclusion as the overall amount of silver ions released by bone cement containing oleic acid capped silver NP is about 10 folds lower than that of tiopronin capped silver NP.<sup>24</sup> This lower silver ion release is probably as consequence of the lower NP concentration in bone cement used in this work.

Small amounts of silver are ingested daily, (minority) some is resorbed by the intestine, the rest (majority) is excreted by the liver; *in vivo* concentrations below 200 ppb are considered normal.<sup>39</sup> The amounts released (2–3 µg/day) from the bone cement in this will likely raise the blood silver level in an adult by less than 20 ppb (even when 10 folds bigger bone cements quantities are used leading to 20–30 µg/day and assuming 2–3 L of blood, the increase of Ag<sup>+</sup> is 10–15 µg/L (ppb); hence we can exclude systemic toxic effects.

Nanoindentation experiments revealed that the mechanical properties of bone cement are quite uniform from the superficial to the bulk area; this also suggests that the NP are homogeneously distributed in the samples. In addition to the nanoindentation experiments, the determination of the compression strength revealed that the materials properties of the bone cement, irrespectively of the presence of oleic acid capped silver NP, decreased with time during immersion in fluids. This is attributed to the uptake of water, as determined in Figure 6; such phenomenon occurs in the first few days and the mass of water containing in the bone cement remains stable after this initial period of time. The water uptake accounting for the change in mechanical properties appeared validated by the simultaneous decrease in Young's modulus as measured through nanoindentation after 24 h and 2 weeks of contact with PBS and increase in water content in the bone cement. After the first 2–3 weeks, the water content reached a plateau and no further changes were detected in Young's modulus through nanoindentation.

To be adopted as a feasible medical device that prevents infections, bone cement containing NP must also possess other properties such as satisfactory mechanical and cytocompatibility characteristics. As our results proved, no detrimental effect resulted from the presence of oleic acid capped silver NP on the mechanical properties of PMMA bone cement determined through nanoindentation and macrocompression strength (Figures 5 and 7). Moreover, the cytocompatibility of the bone samples with encapsulated oleic acid capped silver NP was no different than standard PMMA-based bone cement (Figure 3).

## CONCLUSIONS

Silver NP capped with oleic acid can confer antimicrobial properties to bone cement without influencing its mechanical properties and cytocompatibility.

Concentration of NP as low as 0.05%, w/w allowed a significant reduction of the number of microorganisms (MRSA, *S. aureus*, *S. epidermidis*, and *A. baumannii*) associated to bone cement and orthopaedic surgery related infections. These pathogens are known to be resistant to some antibiotics commonly used in the treatment and prevention of postoperative infections.

This work demonstrated the feasibility of developing antimicrobial bone cement through its impregnation with Ag NP capped with oleic acid offering an alternative to the reliance on antibiotics. As such molecules are quickly losing efficacy through microorganisms developing resistance, a novel solution surpassing this approach to infection is greatly needed.

## REFERENCES

- Ridgeway S, Wilson J, Charlet A, Kafatos G, Pearson A, Coello R. Infection of the surgical site after arthroplasty of the hip. *J Bone Joint Surg Br* 2005;87-B:844–850.
- Edwards JR, Peterson KD, Mu Y, Banerjee S, Allen-Bridson K, Morrell G, Dudeck MA, Pollock DA, Horan TC. National Healthcare Safety Network (NHSN) report: Data summary for 2006 through 2008, issued December 2009. *Am J Infect Control* 2009;37:783–805.
- Gougoulias N, Khanna A, Maffulli N. How successful are current ankle replacements?: A systematic review of the literature. *Clin Orthop Relat Res* 2010;468:199–208.
- Meehan J, Jamali AA, Nguyen H. Prophylactic antibiotics in hip and knee arthroplasty. *J Bone Joint Surg Am* 2009;91A:2480–2489.
- Tyllianakis ME, Karageorgos AC, Marangos MN, Saridis AG, Lambiris EE. Antibiotic prophylaxis in primary hip and knee arthroplasty comparison between cefuroxime and two specific antistaphylococcal agents. *J Arthroplasty* 2010;25:1078–1082.
- Kittinger C, Marth E, Windhager R, Weinberg A, Zarfel G, Baumert R, Felisch S, Kuehn KD. Antimicrobial activity of gentamicin palmitate against high concentrations of *Staphylococcus aureus*. *J Mater Sci Mater Med* 2011;22:1447–1453.
- Kaplan L, Kurdziel M, Baker KC, Verner J. Characterization of daptomycin-loaded antibiotic cement. *Orthopedics* 2012;35:e503–e509.
- van de Belt H, Neut D, Schenk W, van Horn JR, van der Mei HC, Busscher HJ. *Staphylococcus aureus* biofilm formation on different gentamicin-loaded polymethylmethacrylate bone cements. *Biomaterials* 2001;22:1607–1611.
- Ofluoglu EA, Bulent E, Derya AM, Sancar BY, Akin G, Bekir T, Erhan E. Efficiency of antibiotic loaded polymethylmethacrylate rods for treatment of the implant-related infections in rat spine. *J Spinal Disord Tech* 2012;25:E48–E52.
- Nowinski RJ, Gillespie RJ, Shishani Y, Cohen B, Walch G, Gobeze R. Antibiotic-loaded bone cement reduces deep infection rates for primary reverse total shoulder arthroplasty: a retrospective, cohort study of 501 shoulders. *J Shoulder Elbow Surg* 2012; 21:324–328.
- Montanaro L, Speziale P, Campoccia D, Ravaioli S, Cangini I, Pietrocola G, Giannini S, Arciola CR. Scenery of *Staphylococcus* implant infections in orthopedics. *Future Microbiol* 2011;6:1329–1349.
- Zilberberg MD, Shorr AF. Secular trends in gram-negative resistance among urinary tract infection hospitalizations in the United States, 2000–2009. *Infect Control Hosp Epidemiol* 2013;34:940–946.
- Pathak SP, Gopal K. Evaluation of bactericidal efficacy of silver ions on *Escherichia coli* for drinking water disinfection. *Environ Sci Pollut Res Int* 2012;19:2285–2290.
- Kamat PV, Flumiani M, Hartland GV. Picosecond dynamics of silver 423 nanoclusters. Photoejection of electrons and fragmentation. *J Phys Chem B* 1998;102:3123–3128.
- Jana D, De G. Spontaneous generation and shape conversion of silver nanoparticles in alumina sol, and shaped silver nanoparticle incorporated alumina films. *J Mater Chem* 2011;21:6072–6078.
- Vasilev K, Sah VR, Goreham RV, Ndi C, Short RD, Griesser HJ. Antibacterial surfaces by adsorptive binding of polyvinyl-sulphonate-stabilized silver nanoparticles. *Nanotechnology* 2010; 21:215102.
- Deng Y, Sun Y, Wang P, Zhang D, Jiao X, Ming H, Zhang Q, Jiao Y, Sun X. Nonlinear optical properties of silver colloidal solution by in situ synthesis technique. *Curr Appl Phys* 2008;8:13–17.
- Le AT, Tam LT, Tam PD, Huy PT, Huy TQ, van Hieu N, Kudrinskiy AA, Krutyakov YA. Synthesis of oleic acid-stabilized silver nanoparticles and analysis of their antibacterial activity. *Mat Sci Eng C* 2010;30:910–916.
- Henglein A, Giersig M. Formation of colloidal silver nanoparticles: Capping action of citrate. *J Phys Chem B* 1999;103:9533–9539.
- Stevanovic M, Kovacevic B, Petkovic J, Filipic M, Uskokovic D. Effect of poly-alpha, gamma, L-glutamic acid as a capping agent on morphology and oxidative stress-dependent toxicity of silver nanoparticles. *Int J Nanomed* 2011;6:2837–2847.
- Le Guevel X, Spies C, Daum N, Jung G, Schneider M. Highly fluorescent silver nanoclusters stabilized by glutathione: A promising fluorescent label for bioimaging. *Nano Res* 2012;5:379–387.
- Amato E, Diaz-Fernandez YA, Taglietti A, Pallavicini P, Pasotti L, Cucca L, Milanese C, Grisoli P, Dacarro C, Fernandez-Hechavarría JM, Necchi V. Synthesis, characterization and antibacterial activity against gram positive and gram negative bacteria of biomimetically coated silver nanoparticles. *Langmuir* 2011;27:9165–9173.
- Perni S, Hakala V, Prokopovich P. Biogenic synthesis of silver nanoparticles capped with L-cysteine. *Colloids Surf A* 10.1016/j.colsurfa.2013.09.034. Forthcoming.
- Prokopovich P, Leech R, Carmalt CJ, Parkin IP, Perni S. A novel bone cement impregnated with silver-tiopronin nanoparticles: Its antimicrobial, cytotoxic and mechanical properties. *Int J Nanomed* 2013;8:2227–2237.
- Dong X, Ji X, Wu H, Zhao L, Li J, Yang W. Shape control of silver nanoparticles by stepwise citrate reduction. *J Phys Chem C* 2009; 113:6573–6576.
- Yin Y, Li ZY, Zhong Z, Gates B, Xia Y, Venkateswaran S. Synthesis and characterization of stable aqueous dispersions of silver nanoparticles through the Tollens process. *J Mater Chem* 2002; 12:522–527.
- Oliver WC, Pharr GM. An improved technique for determining hardness and elastic modulus using load and displacement sensing indentation experiments. *J Mater Res* 1992;7:1564–1583.
- Prokopovich P, Perni S, Hall RM, Fisher J. Spatial variation of wear on charity lumbar discs. *Acta Biomater* 2011;7:3914–3926.
- Bechert T, Steinrucke P, Guggenbichler JP. A new method for screening anti-infective biomaterials. *Nat Med* 2000;6:1053–1056.
- Panaček A, Kvitek L, Pruček R, Kolář M, Večeřová R, Pizurová N, Sharma VK, Nevěčná T, Zbořil R. Silver colloid nanoparticles: synthesis, characterization, and their antibacterial activity. *J Phys Chem B* 2006;110:16248–16253.
- Grosso MJ, Sabesan VJ, Ho JC, Ricchetti ET, Iannotti JP. Reinfection rates after 1-stage revision shoulder arthroplasty for patients with unexpected positive intraoperative cultures. *J Shoulder Elbow Surg* 2012;21:754–758.
- Sorlí L, Puig L, Torres-Claramunt R, González A, Alier A, Knobel H, Salvadó M, Horcajada JP. The relationship between microbiology results in the second of a two-stage exchange procedure using cement spacers and the outcome after revision total joint replacement for infection: the use of sonication to aid bacteriological analysis. *J Bone Joint Surg Br* 2012;94:249–253.
- Eliopoulos GM, Maragakis LL, Perl TM. *Acinetobacter baumannii*: Epidemiology, antimicrobial resistance, and treatment options. *Clin Infect Dis* 2008;46:1254–1263.
- Tan H, Peng Z, Li Q, Xu X, Guo S, Tang T. The use of quaternised chitosan-loaded PMMA to inhibit biofilm formation and downregulate the virulence-associated gene expression of antibiotic-resistant *Staphylococcus*. *Biomaterials* 2012;33:365–377.
- Alt V, Bechert T, Steinrücke P, Wagener M, Seidel P, Dingeldein E, Domann E, Schnettler R. An in vitro assessment of the



- antibacterial properties and cytotoxicity of nanoparticulate silver bone cement. *Biomaterials* 2004;25:4383–4391.
36. Shi Z, Neoh KG, Kang ET, Wang W. Antibacterial and mechanical properties of cement impregnated with chitosan nanoparticles. *Biomaterials* 2006;27:2440–2449.
  37. Shen SC, Ng WK, Shi Z, Chia L, Neoh KG, Tan RBH. Mesoporous silica nanoparticles-functionalized poly(methyl methacrylate)-based bone cement for effective antibiotics delivery. *J Mater Sci Mater Med* 2011;22:2283–2292.
  38. Van Staden AD, Brand AM, Dicks LMT. Nisin F-loaded brushite bone cement prevented the growth of *Staphylococcus aureus* in vivo. *J Appl Microbiol* 2012;112:831–840.
  39. Ewald A, Hösel D, Patel S, Grover LM, Barralet JE, Gbureck U. Silver-doped calcium phosphate cements with antimicrobial activity. *Acta Biomater* 2011;7:4064–4070.
  40. Sadeghi B, Garmaroudi FS, Hashemi M, Nezhad HR, Nasrollahi A, Ardalan S, Ardalan S. Comparison of the anti-bacterial activity on the nanosilver shapes: Nanoparticles, nanorods and nanoplates. *Adv Powder Tech* 2012;23:22–26.